PAPER

Check for updates

Sc₃N@*Iₕ*-C₈₀ based donor–acceptor conjugate: role of thiophene spacer in promoting ultrafast excited state charge separation†

Rubén Caballero, [ID] [a] Luis David Servián,[a] Habtom B. Gobeze,[c] Olivia Fernandez-Delgado, [ID] [b] Luis Echegoyen, [ID] *[b] Francis D'Souza [ID] *[c] and Fernando Langa [ID] *[a]

Light induced charge separation in a newly synthesized triphenylamine–thiophene-Sc₃N@*Iₕ*-C₈₀ donor–acceptor conjugate and its C₆₀ analog, triphenylamine–thiophene-C₆₀ conjugate is reported, and the significance of the thiophene spacer in promoting electron transfer events is unraveled.

Endohedral metallofullerenes (EMF) are compounds of great interest due to their fascinating structure and unique electronic properties[1–4] which are different from those of empty fullerenes.[5,6] While the early efforts were dedicated to their electronic structure, their chemical functionalization has aroused significant interest in recent years,[7–9] not only to utilize their interesting properties but also to prepare new compounds with potential applications in photovoltaics,[10,11] biomedical[12–15] and materials science applications.[16,17] Due to their higher lowest unoccupied molecular orbital (LUMO) compared to those of empty fullerene cages, EMFs are excellent acceptor materials in organic photovoltaics, capable of increasing the open circuit voltage of the devices.[10] To this end, a few covalent donor–acceptor systems comprising EMFs have been prepared,[8,18–20] which showed the higher stability of the radical-ion pair in comparison with analogous empty fullerenes.[21–31]

Up until now, several methods have been developed to functionalize EMFs such as Diels–Alder,[7,32,33] Bingel–Hirsch reaction,[34–37] cycloaddition with carbenes or benzynes *etc.*[38–41] Among these, 1,3-dipolar cycloaddition of azomethine ylides is perhaps the most used to functionalize EMFs,[38–42] although other dipoles as nitrile imines[43] have been used as well. On the other hand, nitrile oxides react with alkenes to afford 2-isoxazolines and can be prepared from aldoximes by treatment with a chlorinated agent and a weak base, generally (except for hindered nitrile oxides) prepared *in situ* to circumvent dimerization.[44] Cycloadditions of nitrile oxides on fullerenes,[45] carbon

nanotubes[46,47] or graphene[48] are known but only one example of the cycloaddition of a stable nitrile oxide to Sc₃N@*Iₕ*-C₈₀ has been described[49] in an elegant study showing that the isoxazoline ring is fused to a [5,6]-bond junction in the endohedral cage.

Here, we describe the synthesis and photophysical study employing femtosecond transient absorption (fs-TA) spectroscopy, of a donor–acceptor conjugate formed by a triphenylamine moiety as a donor group and Sc₃N@*Iₕ*-isoxazoline-C₈₀ as the acceptor, linked by a thiophene spacer (Fig. 1). The analogous C₆₀ derivative was also prepared for comparison. Here we show that the central thiophene ring promotes π-conjugation between the donor and acceptor entities thus facilitating charge separation processes in these conjugates, useful for optoelectronic applications.
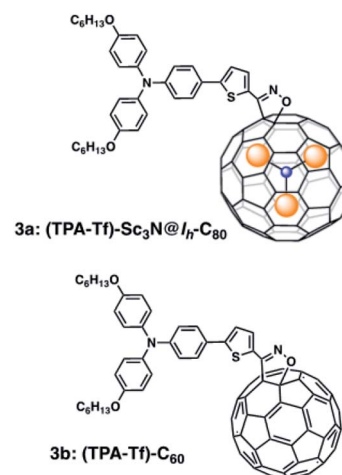

Fig. 1 Structure of the newly synthesized triphenylamine–thiophene-Sc₃N@*Iₕ*-C₈₀ endohedral fullerene conjugate, (**3a**) and its C₆₀ analog derivative (**3b**).

ᵃInstituto de Nanociencia Nanotecnología y Materiales Moleculares (INAMOL), Universidad de Castilla-La Mancha, Campus de la Fábrica de Armas, 45071 Toledo, Spain. E-mail: fernando.langa@uclm.es

ᵇDepartment of Chemistry and Biochemistry, University of Texas at El Paso, 500 W University Avenue, El Paso, Texas 79968, USA. E-mail: luis.echegoyen@utep.edu
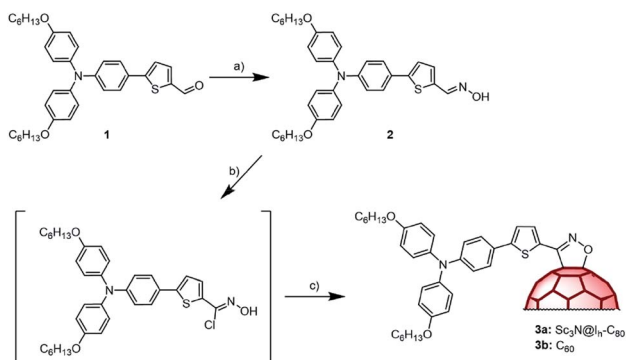
ᶜDepartment of Chemistry, University of North Texas, 1155 Union Circle, Denton, Texas 305070, USA. E-mail: Francis.dsouza@unt.edu

† Electronic supplementary information (ESI) available: Synthesis and experimental details, additional fs-TA spectral data. See DOI: 10.1039/d0ra04379f

Scheme 1 shows the synthetic approach for both donor–acceptor conjugates. Reaction of aldehyde **1**[50] with hydroxylamine hydrochloride in ethanol/pyridine afforded oxime **2**, as a mixture of Z–E isomers, in 77% yield. Then, **2** was reacted with N-chlorosuccinimide (NCS) and after 30 min a solution of $Sc_3N@I_h$-C_{80} in 1,2-dichlorobenzene (o-DCB) and triethylamine was added and stirred for 72 h at room temperature. The progress of the reaction was followed by HPLC, which showed that a new single peak appears as that for $Sc_3N@I_h$-C_{80} disappears. After purification by column chromatography, followed by preparative HPLC, conjugate **3a** was obtained in 25% yield. A similar procedure was followed to prepare the C_{60}-based compound **3b** (see the Experimental section in the ESI for details†). Compound **3a** was characterized by means of MALDI-TOF mass analysis showing the molecular ion peak at 1677.28 amu. The ^1H NMR spectrum contains all the expected signals of the addend. The thiophene H-atoms appear at 7.96 and 7.24 ppm, deshielded compared to those in the oxime due to the presence of the fullerene cage. Note that this signal is broad as a consequence of the hindered rotation. In the ^{13}C NMR spectrum, the most relevant signals are those of the sp^3 C-atoms of the functionalized fullerene cage at 97.7 and 70.3 ppm. Similar features are observed in the spectrum of the C_{60}-based compound **3b**. Finally, the appearance of a broad UV-Vis absorption around 700 nm and the lack of absorption in the 800 nm region, expected for the [6,6]-isomer, confirmed the formation of the [5,6]-isomer; a result that agrees well with the previously described examples of 1,3-dipolar cycloadditions on $Sc_3N@I_h$-C_{80}.[49] Interestingly, **3a** undergoes a fast retro-cycloaddition when refluxed in o-DCB while **3b** is stable under these conditions.

The absorption spectrum of **3a** and **3b** in dichloromethane together with the parent oxime **2** are shown in Fig. 2a. Oxime **2** exhibits a maximum at 390 nm which is red-shifted to 412 nm and 407 nm in cycloadducts **3a** and **3b**, respectively, indicating a stronger influence of the $Sc_3N@I_h$-C_{80} cage when compared to C_{60} over the electronic properties of the organic addend. In the case of **3a**, a band around 690 nm is observed and the spectrum lacked the typical band around 800 nm ascribed to [6,6]-EMF adducts;[51] again confirming the [5,6]-structure for **3a**, as discussed above.
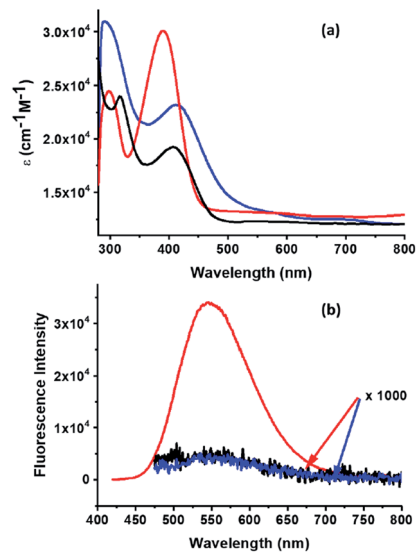

Fig. 2 (a) Absorption and (b) fluorescence spectra of 10^{-6} M solutions of **2** (red), **3a** (black) and **3b** (blue) in CH_2Cl_2.

The photophysical properties of **3a** and **3b** were first studied in dichloromethane by steady-state fluorescence spectroscopy with a 407 nm excitation wavelength (λ_{ex}), which mostly excites the TPA moiety. The model oxime **2** showed strong fluorescence with a maximum at 544 nm. The fluorescence of this chromophore was fully quenched upon connection to the fullerene cages for both **3a** and **3b** (Fig. 2b). It is possible that photoinduced charge separation is the reason for the observed fluorescence quenching (vide infra).

The electrochemical properties of **3a** and **3b**, oxime **2** and pristine $Sc_3N@I_h$-C_{80} and C_{60} were investigated by cyclic voltammetry (CV) and Osteryoung square wave voltammetry (OSWV) and the results are summarized in Table 1. Representative CVs for **3a** and **3b** are shown in Fig. 3a. In the anodic region, the first oxidation potentials of **3a** and **3b**, attributed to the alkoxy-TPA-thiophenyl moiety, are positively shifted by 80 mV and 110 mV, respectively, compared to that for oxime **2** (isostructural with the organic addend of **3a–b**), suggesting the

Scheme 1 Reagents and conditions: (a) hydroxylamine hydrochloride, pyridine; (b) NCS; pyridine (c) Et_3N, $Sc_3N@I_h$-C_{80} or C_{60}, r.t.

Table 1 Redox potentials (in V vs. Fc/Fc^+) determined by OSWV of the processes observed for **2**, **3a–b** and reference fullerenes[a]

	E_{Red}^5	E_{Red}^4	E_{Red}^3	E_{Red}^2	E_{Red}^1	E_{Ox}^1	E_{Ox}^2	E_{Ox}^3
3a	—	-2.23^c	-1.50^c		-0.93	0.29	0.53^b	0.80^b
$Sc_3N@C_{80}$	-2.35	-2.23	-1.72	-1.59	-1.20^b	0.69	—	—
3b	-2.39	-1.97	-1.82^b	-1.50	-1.05	0.32	0.87^b	—
C_{60}	—	-2.36	-1.88	-1.42	-1.03	—	—	—
2	—	—	—	—	—	0.21	0.68^b	0.79^b

[a] Determined by OSWV using o-DCB : acetonitrile (4 : 1) as a solvent. A $Ag/AgNO_3$ (0.01 M) electrode was used as a reference and checked against the Fc/Fc^+ couple on a glassy carbon electrode, Pt was used as counter electrode at 20 °C and 0.1 M tetrabutylammonium hexafluorophosphate as supporting electrolyte with scan rate = 100 mV s^{-1}. [b] Non-reversible process. [c] Value corresponding to the overlap of two reduction processes.
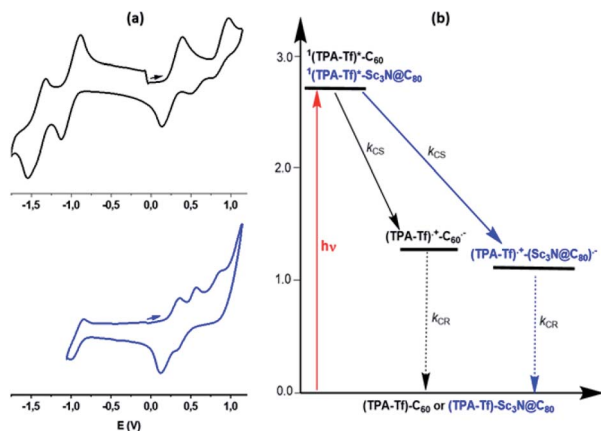
Fig. 3 (a) Cyclic voltammograms of **3b** (black) and **3a** (blue) in *o*-DCB : acetonitrile (4 : 1) (b) energy level diagram showing the different photochemical events occurring for **3a** and **3b** due to TPA excitation. Energies of different states were evaluated from spectral and electrochemical studies. Solid arrows indicate major photo-processes, dashed arrow indicates minor photo-processes. CS = charge separation, CR = charge recombination.

existence of some electronic interactions with the respective fullerene cage. In the cathodic region, the first reduction potential of **3a** is positively shifted by 270 mV when compared to that of pristine $Sc_3N@I_h$-C_{80}. This behavior is similar to what was previously observed for an isoxazoline $Sc_3N@I_h$-C_{80} derivative, confirming the strong influence that functionalization has on the electrochemical properties of the EMF cage.[52] However, the first reduction of **3b** and C_{60} showed similar values (−1.05 V and −1.03 V, respectively) as described in other donor-isoxazolinofullerene derivatives.[44] This behavior is different from that for C_{60} derived pyrrolidinofullerenes, where the first reduction is about 120 mV more negative than for pristine C_{60} as a result of the saturation of one of the double bonds.

From the optical absorption and emission, electrochemical redox potential and structural parameters, Gibbs free-energy changes associated with charge separation (CS) and charge recombination (CR) were estimated according to eqn (i) and (ii)[53]

$$-\Delta G_{CR} = E_{ox} - E_{red} + \Delta G_S \qquad (i)$$

$$-\Delta G_{CS} = \Delta E_{0-0} - (-\Delta G_{CR}) \qquad (ii)$$

where ΔE_{0-0} corresponds to the energy of the ^{1}TPA-Tf* state calculated from luminescence peak maximum at 2.72 eV. The E_{ox} and E_{red} are the first oxidation potential of TPA-Tf and the first reduction potential of the fullerene in the conjugate. The term ΔG_S refers to the electrostatic energy calculated according to the dielectric continuum model. The calculated ΔG_S in *o*-DCB for **3a** and **3b** were found to be −0.09 and −0.11 eV, respectively. Incorporation of these values into eqn (i) and (ii) resulted in ΔG_{CS} and ΔG_{CR} of −1.59 and −1.13 eV for **3a** and −1.46 and −1.26 for **3b**, respectively.

The energy level diagram shown in Fig. 3b was constructed to visualize the possible photochemical events. Excitation of TPA in the dyads leads to a population of its lowest excited singlet

state, ^{1}TPA-Tf*. The ^{1}TPA-Tf* state can undergo a thermodynamically allowed CS to the appended fullerene. The fluorescence spectra in Fig. 2b reveals that attaching $Sc_3N@I_h$-C_{80} or C_{60} to TPA *via* the thiophene spacer leads to quantitative quenching and no new peaks due to fullerene emission suggesting no energy transfer. The data suggest that CS is the most likely quenching mechanism. The high ΔG_{CS} and ΔG_{CR} values and the spatial closeness between the donor and acceptor entities along with the strong electronic coupling by through the thiophene spacer are anticipated to accelerate both the CS and CR processes. Further, fs-TA studies were performed in solvents of different polarity to clarify these predictions. Prior to this, in an effort to spectrally characterize electron transfer products, TPA-Tf (compound **2**) was chemically oxidized using $NOBF_4$ in benzonitrile, as shown in Fig. S11.† Increased additions of the oxidizing agent decreased the intensity of the main peak at 390 nm and resulted in the appearance of new peaks at 375, 486, 564, 731 and 967 nm, corresponding to (TPA-Tf)$^{+\bullet}$. Spectral characteristics of $Sc_3N@I_h$-$C_{80}{}^{-\bullet}$ and $C_{60}{}^{-\bullet}$ with peaks around 1000 nm have been reported earlier.[54,55]

Fs-TA studies were performed in three solvents of varying polarity. Fig. 4 shows fs-TA spectra of **2**, **3a** and **3b** at the indicated delay times in *o*-DCB while those recorded in toluene and benzonitrile are shown in Fig. S12 and S13,† respectively. In all these solvents, immediately after excitation, the instantaneously formed ^{1}**2*** (^{1}TPA-Tf*) revealed a negative peak in the 450–550 nm region due to contributions of ground state bleaching (GSB) and stimulated emission (SE). Positive peaks in the 600 and 1240 nm region due to excited state absorption (ESA) were also observed. With time, the near-IR peak revealed
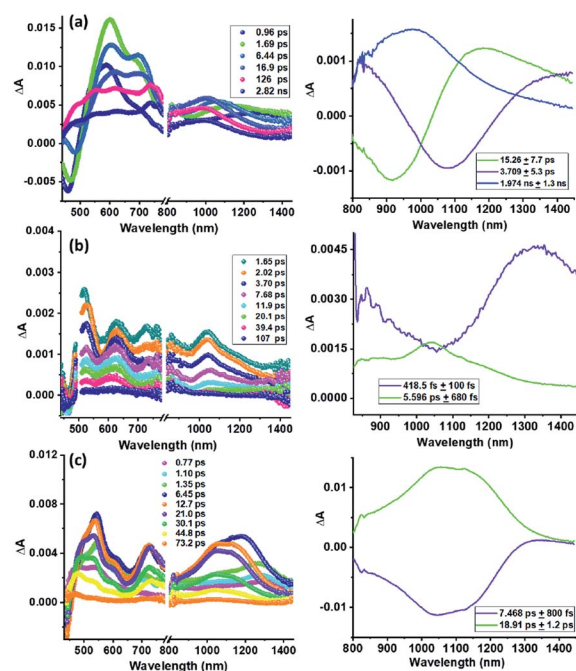

Fig. 4 Fs-TA spectra at the indicated delay times of (a) **2** (λ_{ex} = 390 nm), (b) **3a** (λ_{ex} = 500 nm), and (c) **3b** (λ_{ex} = 390 nm) in *o*-DCB. The DAS are shown in the right hand panels.

Table 2 Time constants and rates for CS and CR for **3a** and **3b**, and earlier reported compounds[54] as a function of solvent polarity

Compound	Solvent	τ_{CS}, ps	k_{CS}, s^{-1}	τ_{CR}, ps	k_{CR}, s^{-1}	Ref.
3a	Toluene	4.4	2.23×10^{11}	65.7	1.50×10^{10}	t.w.
	o-DCB	1.0	10.0×10^{11}	5.6	1.78×10^{11}	t.w.
	PhCN	1.02	9.80×10^{11}	4.3	2.32×10^{11}	t.w.
3b	Toluene	4.2	2.38×10^{11}	732	1.36×10^{9}	t.w.
	o-DCB	7.0	1.43×10^{11}	18	5.56×10^{10}	t.w.
	PhCN	2.9	3.44×10^{11}	6.3	1.59×10^{11}	t.w.
TPA-Sc$_3$N@C$_{80}$	THF	—	3.4×10^{10}		1.7×10^{9}	54
	PhCN	—	—	—	4.5×10^{8}	54
TPA-C$_{60}$	THF	—	7.6×10^{10}		8.0×10^{9}	54
	PhCN	—	—	—	6.5×10^{9}	54

a blue-shift, likely due to solvation or vibrational cooling,[56,57] and at longer delay times, the recovery and decay of negative and positive peaks was associated with emergence of new peaks in the 735 and 1000 nm range likely due to ^{3}**2***, formed *via* intersystem crossing (ISC).

For **3a** and **3b** ultrafast electron transfer events were observed. As shown in Fig. 4b and c, the recovery and decay of peaks corresponding to ^{1}(TPA-Tf)* were rapid with new peaks developing within a few picoseconds characteristic of (TPA-Tf)$^{+\bullet}$-Sc$_3$N@I_h-C$_{80}^{-\bullet}$ in the case of **3a** and (TPA-Tf)$^{+\bullet}$-C$_{60}^{-\bullet}$ in the case of **3b**. These are signature peaks of Sc$_3$N@I_h-C$_{80}^{-\bullet}$ and C$_{60}^{-\bullet}$ in the near-IR region and (TPA-Tf)$^{+\bullet}$ in the visible region. Further, decay associated spectra (DAS) were generated from global analysis to evaluate time constants for CS and CR, as shown in the right-hand panels of Fig. 4. Changing the solvent revealed solvent polarity dependent electron transfer kinetics, showing that polar solvents facilitated the charge separation process. The measured time constants and rates are given in Table 2.

The data presented in Table 2 reveals the following: (i) the k_{CS} values are generally higher for **3a** compared to **3b** which could be attributed to the free-energy changes (see Fig. 3b) where facile charge separation for **3a** over **3b** was noted. (ii) Although some charge stabilization is observed in nonpolar toluene, in general k_{CR} values are also much faster on the order of 10^{10} to 10^{11} s^{-1}. (iii) A comparison of electron transfer rates between the present system and the previously reported TPA-fullerene conjugate[54] where charge stabilization was observed to some extent suggests that the thiophene entity enhances the π-conjugation between the donor and acceptor entities in **3a** and **3b**, thus facilitating electron transfer events in both directions.

Conclusions

In summary, new donor–acceptor conjugates, TPA-Tf-Sc$_3$N@I_h-C$_{80}$, and its C$_{60}$ analog, TPA-Tf-C$_{60}$, were synthesized by a 1,3-dipolar cycloaddition reaction of nitrile oxides. The thiophene unit promotes the π-conjugation between the donor and acceptor entities. An energy level diagram constructed using spectral and electrochemical data revealed an exothermic excited state charge separation, more so for the TPA-Tf-Sc$_3$N@I_h-C$_{80}$ conjugate. Photoexcitation of the TPA-Tf entity in the conjugates promoted charge separation within a few picoseconds, attributed to the π-linker, thiophene, connecting the donor and acceptor units, accesible redox potentials and spatial closeness of the donor and acceptor entities of the conjugates. Further studies to fully explore the potential of the current synthetic methodology to functionalize endohedral fullerenes for photochemical and optoelectronic applications are underway in our laboratories.

Conflicts of interest

Authors declare no conflict of interest.

Acknowledgements

Notes and references

1 N. Shigeru, K. Kaoru and A. Takeshi, *Bull. Chem. Soc. Jpn.*, 1996, **69**, 2131–2142.
2 X. Lu, L. Feng, T. Akasaka and S. Nagase, *Chem. Soc. Rev.*, 2012, **41**, 7723–7760.
3 T. Akasaka and X. Lu, *Chem. Rec.*, 2012, **12**, 256–269.
4 X. Lu, T. Akasaka and S. Nagase, *Chem. Commun.*, 2011, **47**, 5942–5957.
5 A. A. Popov, S. Yang and L. Dunsch, *Chem. Rev.*, 2013, **113**, 5989–6113.
6 L. Dunsch and S. Yang, *Small*, 2007, **3**, 1298–1320.
7 P. Jin, Y. Li, S. Magagula and Z. Chen, *Coord. Chem. Rev.*, 2019, **388**, 406–439.
8 Y. Chai, X. Liu, B. Wu, L. Liu, Z. Wang, Y. Weng and C. Wang, *J. Am. Chem. Soc.*, 2020, **142**, 4411–4418.
9 X. Lu, L. Bao, T. Akasaka and S. Nagase, *Chem. Commun.*, 2014, **50**, 14701–14715.

10 R. B. Ross, C. M. Cardona, D. M. Guldi, S. G. Sankaranarayanan, M. O. Reese, N. Kopidakis, J. Peet, B. Walker, G. C. Bazan, E. Van Keuren, B. C. Holloway and M. Drees, *Nat. Mater.*, 2009, **8**, 208–212.

11 J. R. Pinzón, M. E. Plonska-Brzezinska, C. M. Cardona, A. J. Athans, S. S. Gayathri, D. M. Guldi, M. Á. Herranz, N. Martín, T. Torres and L. Echegoyen, *Angew. Chem., Int. Ed.*, 2008, **47**, 4173–4176.

12 S. Yang, T. Wei and F. Jin, *Chem. Soc. Rev.*, 2017, **46**, 5005–5058.

13 J. W. Meng, D. L. Wang, P. C. Wang, L. Jia, C. Chen and X.-J. Liang, *J. Nanosci. Nanotechnol.*, 2010, **10**, 8610–8616.

14 T. Li and H. C. Dorn, *Small*, 2017, **13**, 1603152.

15 R. D. Bolskar, in *Medicinal Chemistry and Pharmacological Potential of Fullerenes and Carbon Nanotubes*, ed. F. Cataldo and T. Da Ros, Springer Netherlands, Dordrecht, 2008, pp. 157–180.

16 X. Lu, T. Akasaka and S. Nagase, *Acc. Chem. Res.*, 2013, **46**, 1627–1635.

17 M. N. Chaur, F. Melin, A. L. Ortiz and L. Echegoyen, *Angew. Chem., Int. Ed.*, 2009, **48**, 7514–7538.

18 B. Liu, H. Fang, X. Li, W. Cai, L. Bao, M. Rudolf, F. Plass, L. Fan, X. Lu and D. M. Guldi, *Chem.–Eur. J.*, 2015, **21**, 746–752.

19 J. R. Pinzón, C. M. Cardona, M. Á. Herranz, M. E. Plonska-Brzezinska, A. Palkar, A. J. Athans, N. Martín, A. Rodríguez-Fortea, J. M. Poblet, G. Bottari, T. Torres, S. S. Gayathri, D. M. Guldi and L. Echegoyen, *Chem.–Eur. J.*, 2009, **15**, 864–877.

20 Y. Takano, M. Á. Herranz, N. Martín, S. G. Radhakrishnan, D. M. Guldi, T. Tsuchiya, S. Nagase and T. Akasaka, *J. Am. Chem. Soc.*, 2010, **132**, 8048–8055.

21 M. Rudolf, L. Feng, Z. Slanina, W. Wang, S. Nagase, T. Akasaka and D. M. Guldi, *Nanoscale*, 2016, **8**, 13257–13262.

22 D. M. Guldi, *Chem. Soc. Rev.*, 2002, **31**, 22–36.

23 H. Imahori, K. Tamaki, D. M. Guldi, C. Luo, M. Fujitsuka, O. Ito, Y. Sakata and S. Fukuzumi, *J. Am. Chem. Soc.*, 2001, **123**, 2607–2617.

24 D. M. Guldi, M. Maggini, G. Scorrano and M. Prato, *J. Am. Chem. Soc.*, 1997, **119**, 974–980.

25 N. Martín, L. Sánchez, M. Á. Herranz, B. Illescas and D. M. Guldi, *Acc. Chem. Res.*, 2007, **40**, 1015–1024.

26 D. M. Guldi, A. Gouloumis, P. Vázquez and T. Torres, *Chem. Commun.*, 2002, 2056–2057, DOI: 10.1039/b205620h.

27 N. Martín, L. Sánchez, M. A. Herranz and D. M. Guldi, *J. Phys. Chem. A*, 2000, **104**, 4648–4657.

28 S. Fukuzumi, K. Ohkubo, H. Imahori and D. M. Guldi, *Chem.–Eur. J.*, 2003, **9**, 1585–1593.

29 D. M. Guldi, I. Zilbermann, A. Gouloumis, P. Vázquez and T. Torres, *J. Phys. Chem. B*, 2004, **108**, 18485–18494.

30 D. I. Schuster, P. Cheng, P. D. Jarowski, D. M. Guldi, C. Luo, L. Echegoyen, S. Pyo, A. R. Holzwarth, S. E. Braslavsky, R. M. Williams and G. Klihm, *J. Am. Chem. Soc.*, 2004, **126**, 7257–7270.

31 D. I. Schuster, K. Li, D. M. Guldi, A. Palkar, L. Echegoyen, C. Stanisky, R. J. Cross, M. Niemi, N. V. Tkachenko and H. Lemmetyinen, *J. Am. Chem. Soc.*, 2007, **129**, 15973–15982.

32 S. Sato, Y. Maeda, J.-D. Guo, M. Yamada, N. Mizorogi, S. Nagase and T. Akasaka, *J. Am. Chem. Soc.*, 2013, **135**, 5582–5587.

33 S. Osuna, M. Swart and M. Solà, *J. Am. Chem. Soc.*, 2009, **131**, 129–139.

34 N. Alegret, A. Rodríguez-Fortea and J. M. Poblet, *Chem.–Eur. J.*, 2013, **19**, 5061–5069.

35 M. Garcia-Borràs, M. R. Cerón, S. Osuna, M. Izquierdo, J. M. Luis, L. Echegoyen and M. Solà, *Angew. Chem., Int. Ed.*, 2016, **55**, 2374–2377.

36 J. R. Pinzón, T. Zuo and L. Echegoyen, *Chem.–Eur. J.*, 2010, **16**, 4864–4869.

37 N. Alegret, M. N. Chaur, E. Santos, A. Rodríguez-Fortea, L. Echegoyen and J. M. Poblet, *J. Org. Chem.*, 2010, **75**, 8299–8302.

38 B. Cao, T. Wakahara, Y. Maeda, A. Han, T. Akasaka, T. Kato, K. Kobayashi and S. Nagase, *Chem.–Eur. J.*, 2004, **10**, 716–720.

39 Y. Takano, Z. Slanina, J. Mateos, T. Tsuchiya, H. Kurihara, F. Uhlik, M. Á. Herranz, N. Martín, S. Nagase and T. Akasaka, *J. Am. Chem. Soc.*, 2014, **136**, 17537–17546.

40 Y. Maeda, M. Kimura, C. Ueda, M. Yamada, T. Kikuchi, M. Suzuki, W.-W. Wang, N. Mizorogi, N. Karousis, N. Tagmatarchis, T. Hasegawa, M. M. Olmstead, A. L. Balch, S. Nagase and T. Akasaka, *Chem. Commun.*, 2014, **50**, 12552–12555.

41 T. Cai, L. Xu, M. R. Anderson, Z. Ge, T. Zuo, X. Wang, M. M. Olmstead, A. L. Balch, H. W. Gibson and H. C. Dorn, *J. Am. Chem. Soc.*, 2006, **128**, 8581–8589.

42 T. Cai, Z. Ge, E. B. Iezzi, T. E. Glass, K. Harich, H. W. Gibson and H. C. Dorn, *Chem. Commun.*, 2005, 3594–3596, DOI: 10.1039/b503333k.

43 C. Ma, B. Xu, G. Xie, J. He, X. Zhou, B. Peng, L. Jiang, B. Xu, W. Tian, Z. Chi, S. Liu, Y. Zhang and J. Xu, *Chem. Commun.*, 2014, **50**, 7374–7377.

44 K. V. Gothelf and K. A. Jørgensen, *Chem. Rev.*, 1998, **98**, 863–910.

45 F. Langa, P. de la Cruz, E. Espíldora, A. González-Cortés, A. de la Hoz and V. López-Arza, *J. Org. Chem.*, 2000, **65**, 8675–8684.

46 M. Alvaro, P. Atienzar, P. de la Cruz, J. L. Delgado, V. Troiani, H. Garcia, F. Langa, A. Palkar and L. Echegoyen, *J. Am. Chem. Soc.*, 2006, **128**, 6626–6635.

47 M. Vizuete, M. J. Gómez-Escalonilla, J. L. G. Fierro, P. Atienzar, H. García and F. Langa, *ChemPhysChem*, 2014, **15**, 100–108.

48 H. Uceta, M. Vizuete, J. R. Carrillo, M. Barrejón, J. L. G. Fierro, M. P. Prieto and F. Langa, *Chem.–Eur. J.*, 2019, **25**, 14644–14650.

49 L. Bao, M. Chen, W. Shen, C. Pan, K. B. Ghiassi, M. M. Olmstead, A. L. Balch, T. Akasaka and X. Lu, *Inorg. Chem.*, 2016, **55**, 4075–4077.

50 A. Aljarilla, C. Herrero-Ponce, P. Atienzar, S. Arrechea, P. d. l. Cruz, F. Langa and H. García, *Tetrahedron Lett.*, 2013, **69**, 6875–6883.

51 N. Martín, M. Altable, S. Filippone, A. Martín-Domenech, R. Martínez-Álvarez, M. Suarez, M. E. Plonska-Brzezinska, O. Lukoyanova and L. Echegoyen, *J. Org. Chem.*, 2007, **72**, 3840–3846.

52 C. Shu, T. Cai, L. Xu, T. Zuo, J. Reid, K. Harich, H. C. Dorn and H. W. Gibson, *J. Am. Chem. Soc.*, 2007, **129**, 15710–15717.

53 D. Rehm and A. Weller, *Isr. J. Chem.*, 1970, **8**, 259–271.

54 J. R. Pinzón, D. C. Gasca, S. G. Sankaranarayanan, G. Bottari, T. Torres, D. M. Guldi and L. Echegoyen, *J. Am. Chem. Soc.*, 2009, **131**, 7727–7734.

55 C. B. KC, G. N. Lim and F. D'Souza, *Nanoscale*, 2015, **7**, 6813–6826.

56 J. Moreno, A. L. Dobryakov, I. N. Ioffe, A. A. Granovsky, S. Hecht and S. A. Kovalenko, *J. Chem. Phys.*, 2015, **143**, 024311.

57 M. Fakis, P. Hrobarik, O. Yushchenko, I. Sigmundova, M. Koch, A. Rosspeintner, E. Stathatos and E. Vauthey, *J. Phys. Chem. C*, 2014, **118**, 28509–28519.